A Techno-Economic-Environmental Feasibility Study of Residential Solar Photovoltaic/Biomass Power Generation for Rural Electrification: A Real Case Study

Rasha Kassem, Mohamed Metwally Mahmoud, Nagwa F Ibrahim, Abdulaziz Alkuhayli, Usama Khaled, Abderrahmane Beroual, Hedra Saleeb

sustainability

MDPI

Article

A Techno-Economic-Environmental Feasibility Study of Residential Solar Photovoltaic/Biomass Power Generation for Rural Electrification: A Real Case Study

Rasha Kassem [1], Mohamed Metwally Mahmoud [2,*], Nagwa F. Ibrahim [3], Abdulaziz Alkuhayli [4], Usama Khaled [2], Abderrahmane Beroual [5] and Hedra Saleeb [1,*]

[1] Electrical Department, Faculty of Technology and Education, Sohag University, Sohag 82524, Egypt
[2] Electrical Engineering Department, Faculty of Energy Engineering, Aswan University, Aswan 81528, Egypt
[3] Electrical Department, Faculty of Technology and Education, Suez University, P.O. Box 43221, Suez 43533, Egypt
[4] Department of Electrical Engineering, College of Engineering, King Saud University, Riyadh 11421, Saudi Arabia
[5] AMPERE Lab UMR CNRS 5005, Ecole Centrale de Lyon, University of Lyon, 36 Avenue Guy de Collongue, 69130 Ecully, France
* Correspondence: metwally_m@aswu.edu.eg (M.M.M.); hedra_mahfouz@techedu.sohag.edu.eg (H.S.)

Abstract: To avert climate change, there has been a rise in the usage of green energy sources that are also beneficial to the environment. To generate sustainable energy in a financially and technically efficient manner, our research attempts to close the gaps. The potential of green sources like photovoltaic (PV) and biomass for a rural community southwest of Sohag Al Gadida City, Sohag, Egypt, is examined in this research considering its techno-economic (TE) and eco-friendly feasibility. The HOMER Pro v3.14 package is used as a scaling and optimization instrument, to calculate the price of the PV/biomass setup and the size and characteristics of its parts. This is to estimate the corresponding electrical production and reduce the total annual cost for the customer. The suggested system structure is validated through the presentation of simulation outcomes and evaluations utilizing MATLAB/SIMULINK R2022a. In addition, a TE-environmental investigation of the optimized PV/biomass structure is performed. The optimum structure is carefully chosen from the best four configurations using the demand predilection by analogy to the perfect technique based on the generation cost, operation cost, energy production, and renewable fraction. The results also indicate that using hybrid PV/biomass is an attractive choice with the initial capital cost (ICC: USD 8.144), net present cost (NPC: USD 11,026), a low cost of energy (LCOE: 0.184 USD/kWh), and the high renewable fraction (RF: 99.9%) of the system. The annual CO_2 emission performance of a PV/biomass system is much better than that of the grid alone and PV/diesel. This method might be applied in rural areas in other developing countries.

Keywords: techno-economic feasibility; PV/biomass generation; CO_2 emissions; HOMER package; clean energy

Citation: Kassem, R.; Mahmoud, M.M.; Ibrahim, N.F.; Alkuhayli, A.; Khaled, U.; Beroual, A.; Saleeb, H. A Techno-Economic-Environmental Feasibility Study of Residential Solar Photovoltaic/Biomass Power Generation for Rural Electrification: A Real Case Study. *Sustainability* **2024**, *16*, 2036. https://doi.org/10.3390/su16052036

Academic Editor: Idiano D'Adamo

Received: 23 January 2024
Revised: 23 February 2024
Accepted: 24 February 2024
Published: 29 February 2024

1. Introduction

Two major events prompted manufacturing countries to consider new and green energy (GE) as a complement to the expected growth in their national energy needs. These proceedings include the current global energy calamity and the growing awareness of the influence of fossil fuel (FF) emissions on the environment. To mitigate the potential harm caused by these emissions, anti-pollution regulations are currently being discussed and enacted into laws by the governments of industrialized countries [1–3]. One of the major energy sources that contribute to climate change is FFs. The energy information

administration of the US has projected that energy consumption in global markets will increase by 57% from 447 quadrillion British Thermal Units (BTUs) in 2004 to 702 quadrillion BTUs in 2030 [4,5].

The globe's population is growing at a fast rate, which is the primary driver of this rise. The fact that there currently exist over seven billion individuals on Earth and that number is predicted to grow by one billion every 12 years makes finding a remedy to this issue challenging [6]. There is a boost in the search and exploitation of GE sources due to the rise in global energy utilization (EU). In a century, the accessibility of fossil fuel-based energy might not be able to keep up with the constant rise in the EU [6,7]. Increasing the availability of GE forms is therefore a very attractive approach. To substitute conventional FFs, scientists and policymakers are searching for alternative GE sources like PV, wind power, biomass, and tidal power. Since GE forms are clean, kind to the environment, and help stop climate change, they are seen as one of the primary solutions to this issue. Many research projects and studies related to GE are being implemented by researchers in this field [8].

Accordingly, the most important research contributions of this paper are as follows:

1- It provides a first-of-its-kind comparison of on/off-grid PV/biomass power generation to meet the electric load of residential buildings for rural electrification in Egypt.
2- It conducts a feasibility study for an HGEF using HOMER Pro software and arrives at an optimal solution.
3- Economic and microeconomic parameters based on the real market of Egypt are used, except for the default values in the HOMER Pro software.

2. Literature Analysis

Among the various GE projects being implemented around the planet, PVs hold great promise [9–12]. PV is a green energy technology that supports household electricity utilization. Getting energy from the sun at a price that is profitable, or even beneficial, as compared to other GE sources, is the overarching objective of photovoltaic innovation. In certain environments, PV power generation has become feasible; nevertheless, due to its widespread use in remote areas, numerous constraints must be investigated from an official, practical, and financial standpoint [13–15]. Compared with traditional technologies, PV technology has obvious environmental advantages in terms of energy generation. PV systems operate quietly and do not emit toxic gases or greenhouse gases (GHGs). PV power generation is an emission-free process. However, the common drawback of all solar power systems is that the production hinges on the availability of PV radiation [16–18]. However, the countries of the Middle East, especially Egypt, are among the countries with the highest accessibility of solar radiation throughout the year, which gives them a competitive advantage over other countries, as shown in Figure 1 [19].

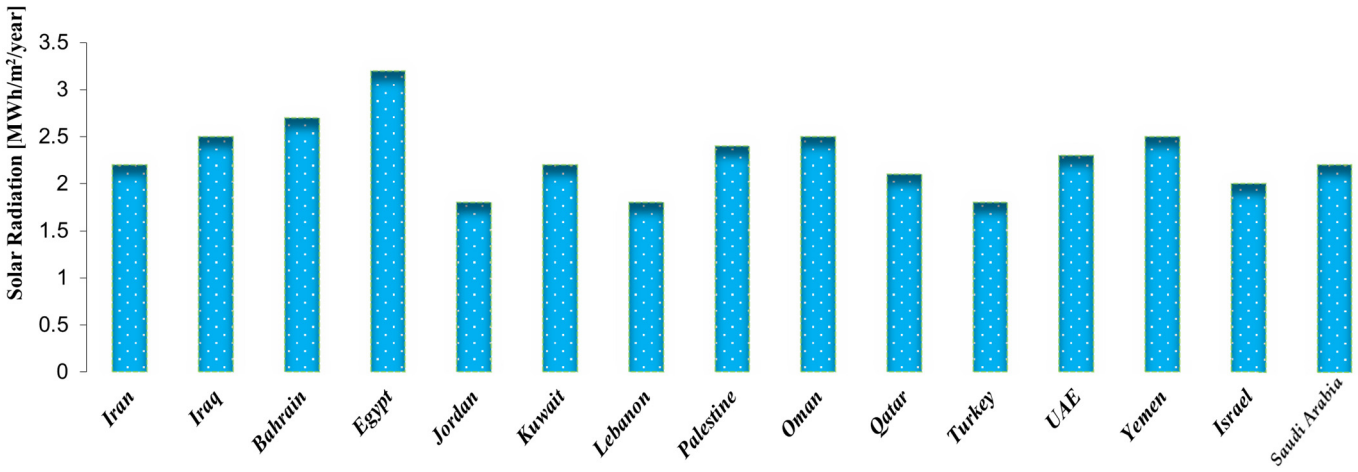

Figure 1. Annual mean solar radiation of the Middle Eastern countries.

GE production in Egypt has made remarkable progress over the past five years; this contributes to saving fuel and reducing the import bill while continuing to reduce carbon emissions. Egypt intends to raise the share of electricity production from GE sources in the power production mix to at least 42% by 2035, compared to 20% in 2023, according to data seen by the Energy Research Unit [20]. The state launched the National Project for Egyptian Rural Development in 2019 to help the neediest rural communities to develop, eliminate poverty, and create job opportunities, in order to provide a decent and sustainable life for citizens. The development of rural areas (RAs) depends heavily on electricity, as it is the driving force for any economic growth. In RAs, most persons face issues related to frequent power outages and meager power quality because the traditional grid is far from the specific location. Hence, a stable and superior electricity feed is crucial and essential to support sustainable expansion. Hence, energy challenges in such areas can be solved by implementing a microgrid power system (MGPS) [21].

This work offers a design of an off-grid hybrid green energy farm (HGEF) to provide electric power for a residential house in an RA, as shown in Figure 2. The off-grid HGEF system is suitable for RAs and remote locations where grid connectivity is difficult to integrate or where the grid is unstable. The off-grid HGEFs can also be made completely self-reliant by incorporating more battery capacity. Planned load profiles and PV system design utilizing HOMER Pro software are included in the system, which consists of PV panels, a biomass generator, batteries, and a converter that regulates electricity flow between the AC and DC buses. An off-grid HGEF requires more initial cost when compared to a grid-connected HGEF system, but it saves energy even when sunlight is not available [22]. The main benefits of the off-grid HGEFs are as follows: it is an environmentally friendly energy source; it is a completely independent system, which does not require traditional grid supplies to function; extra energy is kept in the battery for several days; it is best suited for RAs where the grid is placed at difficult locations such as in mountains or several islands; no government permissions or approvals are required for standalone systems; no power outages take place due to traditional grid failure; the energy stowed in the battery is used in the night; and it is the best replacement for diesel generators. As a result, a thorough analysis of earlier research using the HOMER Pro program was carried out in this field to identify the shortcomings that needed to be rectified with further advancements. A flow chart illustrating the overall methodology is shown in Figure 3. To address the demand for RAs, Table 1, as shown in Appendix A,

highlights prior pertinent works produced in the past five years on optimal HGEF design and techno-economic-environmental analysis utilizing the HOMER Pro program [23,24].

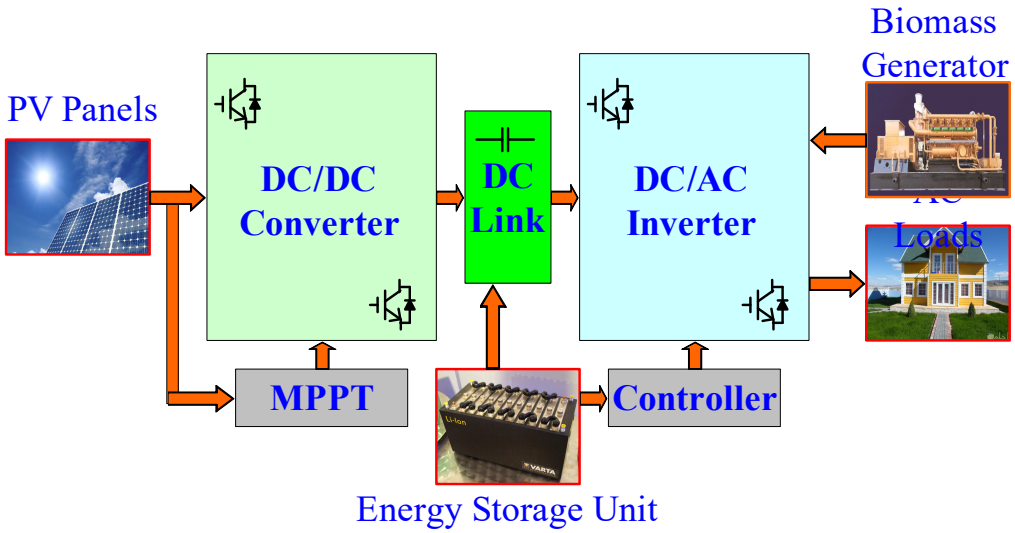

Figure 2. General schematic diagram of the investigated configuration.

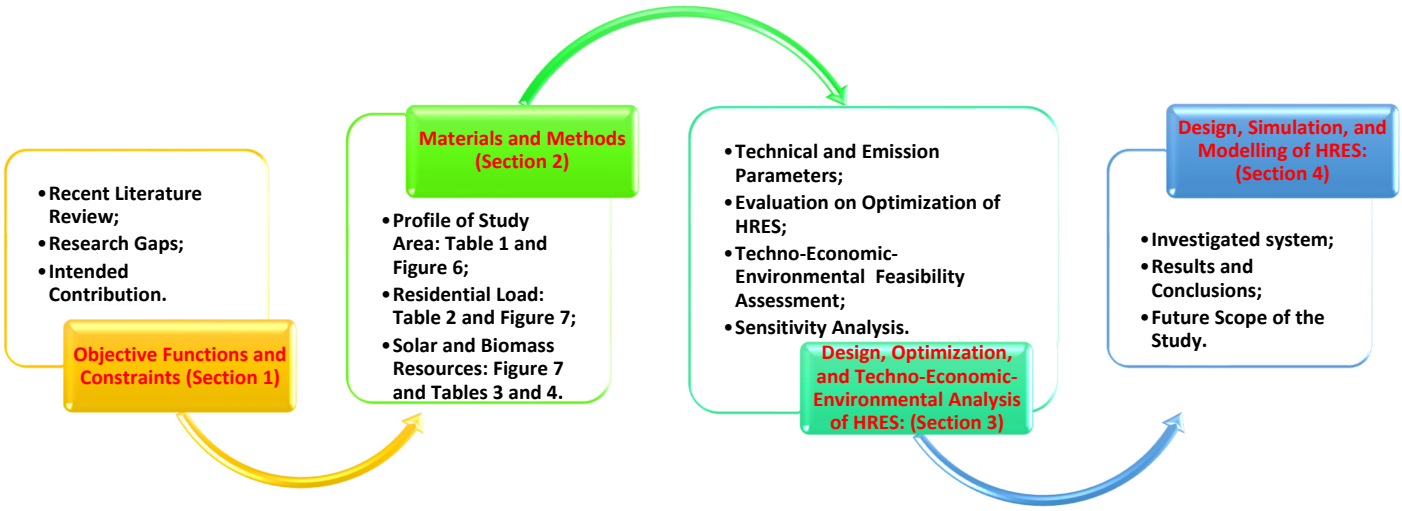

Figure 3. HRES overall methodology flow chart.

Table 1. Average monthly values of daily solar radiation over Sohag Al Gadida City.

Month	Clearness Index	Daily SR * [kWh/m²/Day]	Daily Temperature ** [°C]
January	0.593	3.850	12.420
February	0.657	5.020	14.090
March	0.675	6.150	18.240
April	0.670	6.940	23.680
May	0.666	7.370	28.100
June	0.720	8.130	30.390
July	0.710	7.910	31.210
August	0.709	7.500	30.810
September	0.709	6.740	28.580

October	0.685	5.520	24.640
November	0.630	4.240	18.840
December	0.584	3.570	13.980

* NB: Monthly averages for global horizontal SR over 22 years (July 1983–June 2005). ** NB: Monthly averages for air temperature over 30 years (January 1984–December 2013).

Based on the literature survey of previously published works mentioned in Appendix A, the following can be observed:

- By reviewing most of the previously published works, the PV/biomass renewable integration system has not yet been evaluated in Egypt.
- To enhance the HGEF in Egypt, no thorough TE-environmental assessment based on weather information has been carried out.
- There is no comprehensive comparison of HGEF based on TE-environmental factors, determining whether the on-grid or off-grid mode of operation represents the most cost-effective solution.

This paper is organized as follows: Sections 1 and 2 present an overview of the literature review and theoretical background, including research contributions. Section 3 explains the methodology applied in designing and sizing the PV/biomass system, including study site selection and load evaluation. Section 4 illustrates the TE-environmental investigation of the addressed system, a summary of all components, and a sensitivity analysis. Section 5 provides the design of the HGEF and the outcomes of simulation and modeling implementation usng SIMULINK/MATLAB software. Finally, Section 6 addresses the conclusions.

3. Off-Grid PV/Biomass System Design

This section presents the feasibility study criteria and PV/biomass system sizing.

3.1. Solar Radiation in Egypt

The solar charts indicate that Egypt is one of the republics in the Sunbelt that relishes a high intensity of direct solar radiation (SR), as the typical SR ranges between 2000 and 3200 MWh/m²/year. Sunshine lasts from 9 to 11 h with a few overcast days throughout the year [25]. Solar energy (SE) shows high energy generation potential, reaching an economic potential of about 74,000 TWh/year [26–28]. Egypt's solar map is shown in Figure 4.

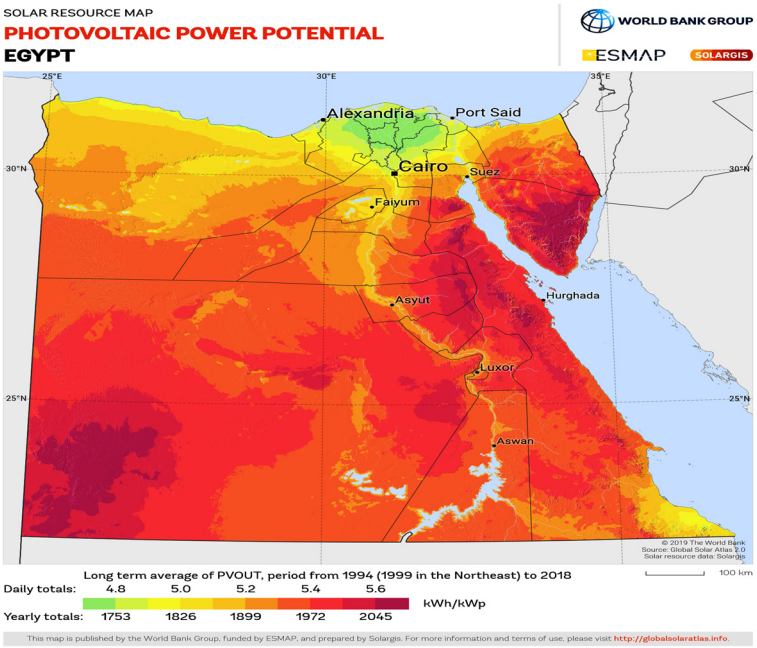

Figure 4. Yearly mean direct SR over Egypt [25].

3.2. Site Location

The proposed location for this case study is a rural village located southwest of Sohag Al Gadida City, Sohag, Egypt. Sohag Al Gadida City is located at 26°26′08″ N latitude and 31°40′19″ E longitude; it is also about 61 m above sea level, as shown in Figure 5. The SR weather can vary from urban to RAs [29,30]. Therefore, knowing the SR climate in the region is vital for determining the performance and sizing of systems.

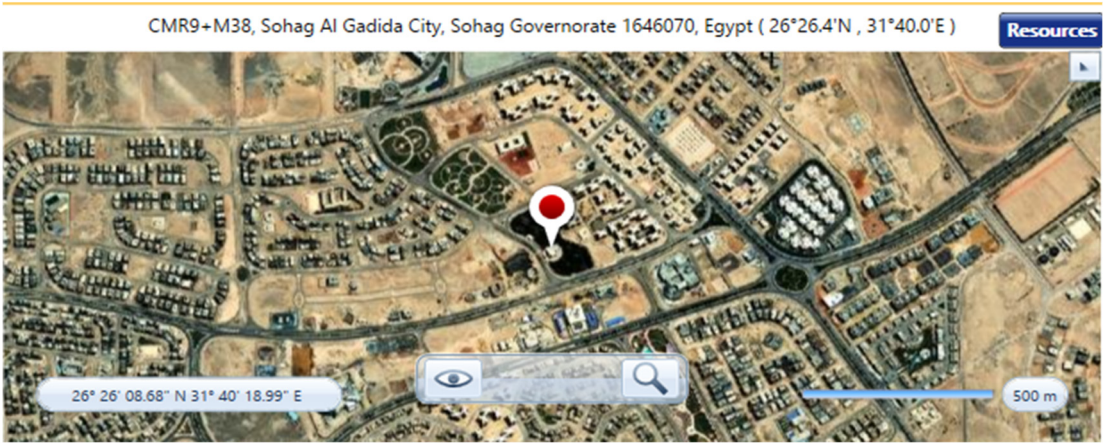

Figure 5. Map of Sohag Al Gadida City, Egypt.

3.3. SR Data for the Site

The "insolation value" refers to the quantity of usable sunshine that the panels can receive on a typical day in the least favorable month of the year. For evaluation, the most challenging month is chosen to make sure that the system will function all year long. In Sohag Al Gadida City, in December, the median daily sunlight is 6 h. An alternative way to comprehend the sunshine figure is as kWh/day of SE coming on each m² of PV panels at a latitude tilting [31]. SR data for the proposed site were obtained from the NASA Surface Meteorology and SE Database website. Table 1 shows the typical monthly values of global SR over Sohag Al Gadida City [32]. The chart shows that there are a lot of SE events at this location, particularly in the summer, when the mean daily SR in June was 8.13 kWh/m²/day [33,34]. Moreover, Figure 6 displays the monthly mean of the horizontal radiation for 22 years.

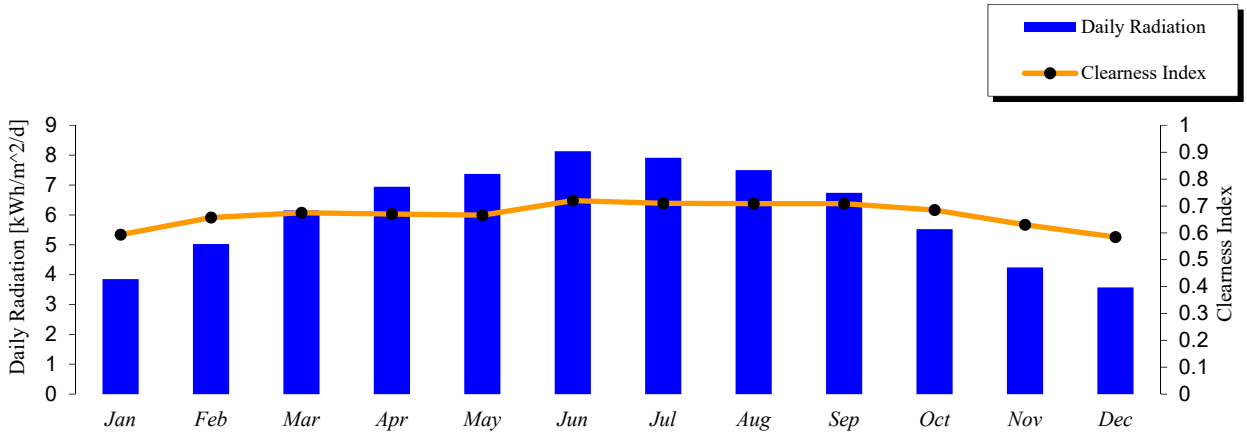

Figure 6. Monthly averages of global horizontal solar radiation data in the selected region.

3.4. Load Data Analysis

The "bottom-up" strategy, which anticipates each daily load and adds them together to get an average daily total, is the recommended way for calculating PV system loads (Figure 7). This approach is straightforward for PV systems intended to supply basic loads like lights, TVs, satellite receivers, laptops, refrigerators, fans, and other appliances. Summer lasts for eight months, from March to October, whereas winter lasts for four months, from November to February. The suggested design process will be based on Table 2, which lists the average daily electrical consumption (EC) of various household appliances (such as lights, televisions, laptops, refrigerators, fans, and other loads). The household's typical daily total load demand is approximately 2733 W. Nevertheless, as Figure 7 illustrates, these loads only operate momentarily rather than continuously.

Table 2. Daily electrical consumption of various appliances in the home.

Devices	Number of Devices	Power [W]	Daily Operating Time [h/d]	Average Daily EC [Wh]
Indoor lighting	10	12	12	1440
Outdoor lighting	5	18	6	540
Ceiling fan	4	50	10	2000
Refrigerator	1	50	24	1200
TV and sat-receiver	2	65	12	1560
Laptop	2	20	6	240
Phone chargers	3	18	1	54
Electric stove	1	500	1	500
Water heater	1	500	1	500
Washing machine	1	1000	2	2000
Other loads	-	500	1	500
Total		2733		10,534

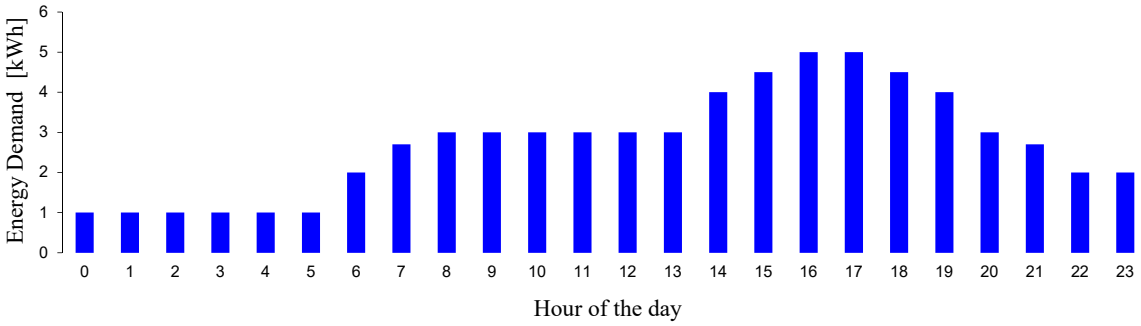

Figure 7. Energy demand daily profile.

Lastly, a normal day's estimation of each load in the house must be made and added up, as indicated in Table 2. The power usage (kWh/day) for each type of load in the house for each of the four seasons was calculated to create the daily load profiles. In comparison with the other seasons, summer has the greatest energy use (12.691 kWh/day).

3.5. PV Array Selection

PV solar panels are the only source to cover the daily energy demand of a home. So the PV module should be carefully selected according to several points. First, the PV

module must have high efficiency, especially in the worst conditions. Also, solar insolation data should be collected according to the site and analyzed so that the design works effectively. Finally, a high-quality PV module must have a low degradation level to prevent energy loss during its lifetime of operation. Table 3 shows the main characteristics of the selected PV module. PV power output is dependent on solar irradiation (I_t) and the PV cell surface temperature (T_C) as follows [35]:

$$P_{PV(t)} = P^*_{PV(STC)} \times f_{PV} \times \frac{I_{(t)}}{I^*_{(STC)}} \times \left[1 + \alpha_{PTC}(T_{C(t)} - T^*_{C(STC)})\right] \quad (1)$$

The symbols $P^*_{PV,}$ $f_{PV,}$ $I_{(t),}$ $I^*_{(STC)}$, $\alpha_{PTC,}$ and $T^*_{C(STC)}$ are the PV array rated capacity (W), derating factor (%), SR incident on the surface (W/m^2), incident SR, power temperature coefficient (%/°C), and surface temperature, respectively.

$$T_{C(t)} = T_{a(t)} \times I_{(t)} \times \frac{T_{C(NOCT)} - 20}{0.8} \times \left[1 - \frac{\eta_{MPP}}{0.9}\right] \quad (2)$$

The symbols $T_{a(t),}$ $T_{C(NOCT)}$, and η_{MPP} are the ambient temperature (°C), normal operating cell temperature (°C), and the efficiency at the MPP (%), respectively.

$$\eta_{MPP} = \eta_{MPP(STC)} \times \left[1 + \alpha_{PTC}(T_{C(t)} - T_{C(STC)})\right] \quad (3)$$

Table 3. Main characteristics of the selected PV module.

Parameters	Values
Max. rate power	250.29 W
Voltage at MPP (V_{mpp})	30.9 V
Current at MPP (I_{mpp})	8.1 A
Open circuit voltage (V_{oc})	36.6 V
Short circuit current (I_{sc})	8.75 A
Total energy of the array (E_t)	12.691 kWh/day
Peak power of the array (P_p)	2.7 kW
Total number (TN) of modules (N_m)	20
TN of cells in series (N_s)	2
TN of cells in parallel (N_p)	10

3.6. Biomass Generator (BG) Selection

A 5-kW biomass generator, coupled with PV arrays, was chosen to satisfy the energy need (EN) of the residential home, due to the PV modules' ability to fulfill EN over the daytime and produce no power at nighttime. In this instance, the EN is met by the biomass generator. The chosen BG can produce 2719 kWh of electricity annually at a constant generation cost of 0.633 USD/kWh, with a capacity factor of 3.1% and a load ratio of at least 25% [36]. Table 4 shows the main characteristics of the selected BG.

Table 4. BG input variables for biogas.

Parameters	Value
Fuel	Biogas
Available biomass	0.1 Tonnes/day
Average price	0.001 USD/Tonne
Carbon content	55%

Density of biogas	1.2 kg/m^3
LHV of biogas	5.50 MJ/kg
Gasification ratio	0.70 kg/kg
Fuel curve (FC) intercept	0.480 kg/h
FC slope	0.297 kg/h/kW

3.7. Battery Bank (BB) Selection

The BB is one of the most vital components necessary to store electrical energy in off-grid PV systems. It is used later in periods of reduced or no seclusion (at night). Furthermore, the BB must be adequately sized as it is the only source that is cast to feed a given load. If the BB is not sized correctly, loads will not be supplied with reliable power and will experience significant outages during the life of the system. Table 5 shows the main conditions of the selected BB.

Table 5. Main specifications of the selected BB.

Parameters	Value
BB type	Lithium-ion
Nominal BB capacity	100 Ah
Nominal BB voltage (V_b)	12 V
Days of autonomy (DOA)	24 h
Charging/discharging cycles	3000
Depth of discharge (DOD)	80%
Round-trip efficiency of batteries (RTE)	85%
TN of BBs in parallel (N_{bp})	6
TN of BBs in series (N_{bs})	4
TN of BBs (N_b)	24

3.8. Solar Inverter (SI) Selection

The SI needs to be able to grip the maximal electrical power that all electrical loads can draw when operating all at once. The total maximum power required = 5000 W, as shown in Figure 7. However, it is almost impossible to run all loads at the same time. Thus, the required SI size will be selected as shown in Table 6.

Table 6. Main specifications of the carefully chosen SI.

Parameters	Value
Max. PV output power	5 kW
Max. output current protection	20 A
BB voltage	48 V
Max. charge current	75 A
Input AC voltage range	100–230 VAC
AC output voltage	100/110/220/230 VAC
SI efficiency	98%

3.9. Charge Controller (CC) Selection

For this system, the MPPT charge controller will be selected based on several criteria. Firstly, the charge controllers must adjust the voltage and current approaching from the PV panels that must be pumped into the BB to avert charging the BB too much and spread the operational life of the BB. Secondly, the CCs must be able to handle the maximum current that comes from the PV array. Finally, the rated power of the CC must be adequately greater than the maximum conceivable power produced by the PV array. Table 7 lists the specifications associated with the CC.

Table 7. Main specifications of the carefully chosen CC.

Parameters	Value
CC manufacturer	Sunny island
CC type	MPPT
Nominal voltage	180–230 V
Max. continuous power	2500 W
Input voltage range	110–230 V
BB capacity	100 Ah
Max. BB charging current	75 A
BB voltage range	36–60 V
CC efficiency	95%

4. Techno-Economic (TE)-Environmental Analysis (EA)

In this part, the TE-EA of a 5 kW off-grid PV/BG as implemented in the HOMER Pro simulator is described. To estimate the performance of on/off-grid PV/BG, programs like HOMER, RET Screen, PV system, etc., are used [37,38]. HOMER Pro software provides a way to assist in the design of the most cost-effective power system built on the proportions of each component in the system and the power source data. HOMER also allows for the comparison of a wide range of design possibilities chosen for their scientific and financial viability. The suggested system as it appears in the HOMER Pro simulator is depicted in Figure 8. An isolated PV system is made up of PV panels, a BG, a SI, CCs, and BB. This configuration delivers electrical energy to the load at the lowest NPC [31]. Table 8 also shows the optimization results against its life cycle cost.

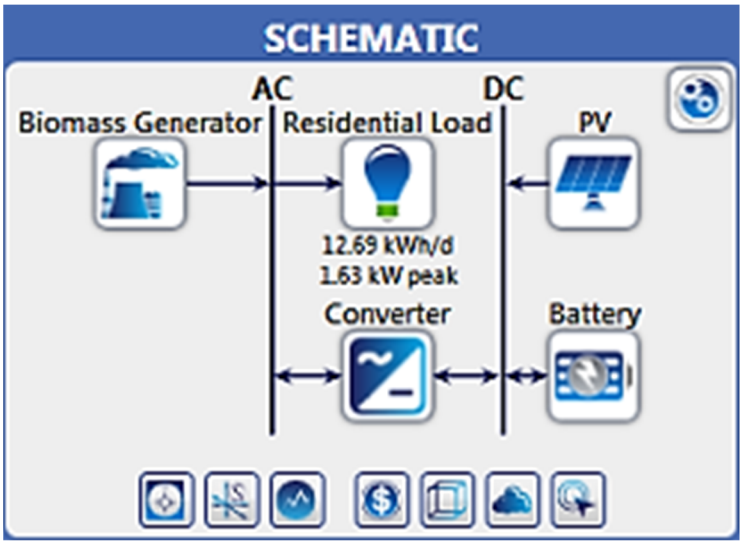

Figure 8. HOMER implementation of an off-grid hybrid PV/biomass system.

Table 8. The optimization results of HOMER.

Architecture				Cost				System		Biomass Generator		
PV (kW)	BG (kW)	Battery (Number)	Converter (kW)	NPC (USD)	COE (USD)	OC (USD/Year)	ICC (USD)	RF (%)	TF (L/Year)	Hours	Production (kWh)	Fuel (L)
5.75	……	15	1.66	USD 10.332	USD 0.173	USD 203.88	USD 7.696	100	0	……	……	…….
5.94	1.5	15	1.83	USD 11.026	USD 0.184	USD 225.26	USD 8.114	99.9	2.40	2	3	2.40
……	1.5	5	1.5	USD 486.637	USD 8.13	USD 37.493	USD 1.950	0	3.995	3.329	4.994	3.995
39	1.5	……	1.87	USD 751.342	USD 12.55	USD 56.247	USD 24.213	0	5.974	4.978	7.467	5.974
……	1.5	……	……	USD 1.27 M	USD 21.22	USD 98.283	USD 250	0	10.512	8.760	13.140	10.512

Biomass generator: BG; Net present cost: NPC; Cost of energy: COE; Operating cost: OC; Initial capital cost: ICC; Renewable fraction: RF.

4.1. Technical Feasibility Assessment

Solar panels are highly susceptible to shadowing. Then, in PV array (PVA) installation, it is crucial to avoid being in the shadows, according to a technical study. A solar module is made up of many PV cells that are linked in series with metallic objects to produce a voltage that can be used. The other cells will have to lower their power to match the PV cell's output if it loses power as a result of shade. Stated differently, there is no distinction between the cell and PV module halves. The PVA needs to be oriented correctly, that is, south at an angle equal to the latitude of the area, to receive the maximum amount of solar energy possible over the year. Generally speaking, PV panels should be horizontally inclined with a slope that is 15° higher than the longitude to work better during the winter. Conversely, the inclination angle of the PV panels should be 15° less than the longitude if the PV system is to be utilized in the summer, which is the best strategy for enhancing the summer efficiency of the PV panels [39,40]. The amount of SR that reaches the solar PVA in a day at the ideal angle can be used to calculate the sunlight period of the solar PVA intended for a residential setting:

$$t = \frac{\theta \times E_s}{1000 \times {W}/{m^2}} \tag{4}$$

The symbols t, θ, and E_S are the sunlight period of the panel (h), optimal angle (°), and SR energy (W/m²), respectively.

Based on the greatest current and BB voltage that the PVA generates at 25 °C, the greatest amount of power that the array can produce may be calculated. The following is one way to put this:

$$P_{PV} = I_{PV(max)} \times V_B \tag{5}$$

where P_{PV}, $I_{PV(max)}$, and V_B are the maximal power (W), maximum current (A), and battery voltage (V), respectively.

The length of the PVA's lighting and the highest electrical output accessible determine how much energy the array can produce each day:

$$E_{PV} = P_{PV} \times t \tag{6}$$

where E_{PV} is the amount of electricity (Wh).

The PVA's energy-gathering capacity declines in proportion to the PV technique's technology efficacy:

$$\eta_e = \eta_i \times \eta_{ccd} \times \eta_b \times \eta_{ca} \tag{7}$$

where η_e , η_i , η_{ccd} , η_b , and η_{ca} are the efficiency of the equipment, inverter, CCdevice, BB, and the cable.

The temperature outside has an impact on the PV cell's efficacy. Values acquired in a laboratory setting at a fixed temperature of 25 °C are used to calculate catalog data for PVA efficacy. The nominal operating cell temperature (NOOCT) of the PV cell is the temperature at which it operates in laboratory trials. A temperature difference of 20 °C between the PVA and the surrounding air is sufficient. The PVA's functioning temperature can be determined using Equation (8) in a variety of ambient temperature conditions.

$$T_p = T_a + (T_{NOCT} + 20) \tag{8}$$

where T_P is the PV panel temperature (°C), and T_a is the ambient temperature (°C).

The following formulas illustrate how a temperature differential can affect the voltage and current values that a PVA can produce:

$$V_{ocv\,2} = V_{ocv} - \Delta T \times 0.0842 \tag{9}$$

$$I_{scc\,2} = I_{scc} - \Delta T \times 0.0086 \tag{10}$$

where V_{ocv} is the open-circuit voltage (V) and I_{scc} is the short-circuit current (A).

The efficacy of the PVA is calculated using the following equation:

$$\eta_{PV\,array} = \frac{V_{ocv\,2} \times I_{scc\,2}}{V_{ocv} \times I_{scc}} \tag{11}$$

Despite being positioned at the ideal angle, the PVA receives changing angles of sunlight throughout the day. Consequently, when the angle deviates by 15° from the optimal angle, the PV system's efficacy drops by 5%. The following formula establishes the PV system's total efficacy:

$$\eta_{te} = \eta_{ea} \times \eta_p \times \eta_e \tag{12}$$

where η_{te} and η_{ea} are the total efficiency of the PV system and the efficiency of the angle inclination.

When calculating the total number of PV modules needed, the highest possible output needs to be considered. The following formula can be used to calculate the necessary quantity of solar PV modules to satisfy the energy requirements of such a system:

$$n_{PV} = \frac{E_r}{E_{PV} \times \eta_{te}} \tag{13}$$

where n_{pv} is the number of PV modules, and E_r is the amount of energy required (Wh).

4.2. Economic Feasibility Assessment

The following equations are utilized in the model for evaluating a system's net present cost (NPC), cost of energy (COE), and operational cost (OC) for financial evaluation. NPC is calculated as the total lifespan current expenditures of the system less the actual value of the earnings generated by the system [41]. As seen in Figure 9, current costs consist of capital costs, operation and maintenance (O and M) costs, and replacement costs (RC). As a result, the suggested technique only generates salvage profit for the duration of the gadget's life. The total annual cost (TAC), which can be found using the following calculation, must be ascertained before the price of COE is known.

$$TAC = CRF_{(i,n)} * NPC \tag{14}$$

where *CRF* attitudes for capital recovery factor are determined by Equation (15).

$$CRF_{(i,n)} = \frac{i \times (1+i)^n}{(1+i)^{n-1}} \quad (15)$$

where i is the annual real discount rate, as calculated in Equation (16), and n is the year's number.

$$i = \frac{i' - f}{1+f} \quad (16)$$

where i is the token discount rate, i' is the rate at which we can pirate cash, and f is the price rise rate. Afterwards, using TAC and energy aided (E_{served}), the COE per kWh formed by the system is calculated using Equation (17).

$$COE = \left(\frac{(TAC/yr)}{E_{served}(\frac{kWh}{yr})} \right) \quad (17)$$

In addition to COE and NPC, one other crucial energy system statistic is OC, which is the yearly total of all expenses and income, excluding annual capital costs, which are calculated by multiplying ICC by the capital recovery factor (CRF). For each component, NPC calculations are carried out using additional equations in HOMER Pro in accordance with Equations (3) to (5); it is advised to consult the HOMER Pro instruction manual [42]. Because BGs require more fuel than other HRES components, their running costs may be greater. At 250 USD/kW, batteries are the most expensive to replace. Based on Figure 9 and Table 9, which illustrate the same overall life period for the project and PV, a substitute cost of PV is USD 225.26.

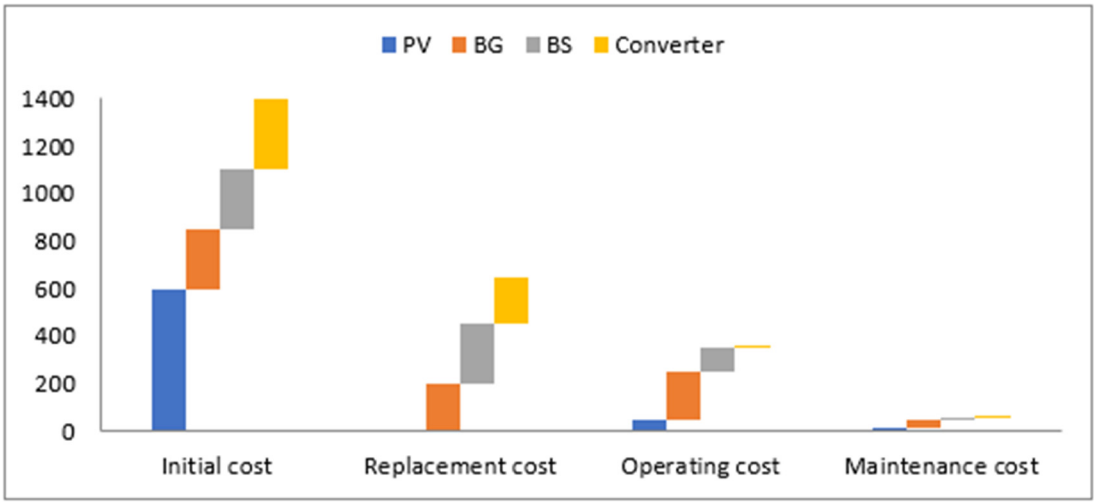

Figure 9. Different current costs for each HGEF component.

Table 9. TE-environmental parameters.

HGEF Components	Parameters	Value	Unit
PV	Lifetime	25	y
	Hours of operating	4366	h/y
	Initial cost	600	USD/kW
	Replacement cost	0	USD/kW

	O and M cost	0.01	USD/kW/y
	CO_2 emission	0.0225	kg/kWh
	Operation temperature	45	°C
	Efficiency	17.3	%
BG	Lifetime	216,000	h
	Hours of operating	603	h/y
	Initial cost	250	USD/kW
	Replacement cost	200	USD/kW
	O and M cost	0.59	USD/kW/y
	Fixed generation cost	0.633	USD/h
	CO_2 emission	0.88	kg/kWh
BB	Lifetime	10	y
	Expected life	150,000	kWh
	Initial cost	250	USD/kW
	Replacement cost	250	USD/kW
	O and M cost	0.01	USD/kW/y
	CO_2 emission	0.028	kg/kWh
	Efficiency	85	%
Converter	Lifetime	15	Y
	Hours of operating	8157	h/y
	Initial cost	300	USD/kW
	Replacement cost	200	USD/kW
	Efficiency	98	%

4.3. Environmental Feasibility Assessment

As illustrated in Figure 10, the GHG pollution of the HGEF is assessed using both on- and off-grid methodologies. To accomplish this, the total yearly GHG pollution is calculated using the formula below [40]:

$$GHG = EM_j * \sum_{t=1}^{8760} P_j(t) \quad (18)$$

The symbols j, EM_j, and P_j are the resource ranking, total CO_2 emissions (in kg/kWh), and energy produced per resource, respectively.

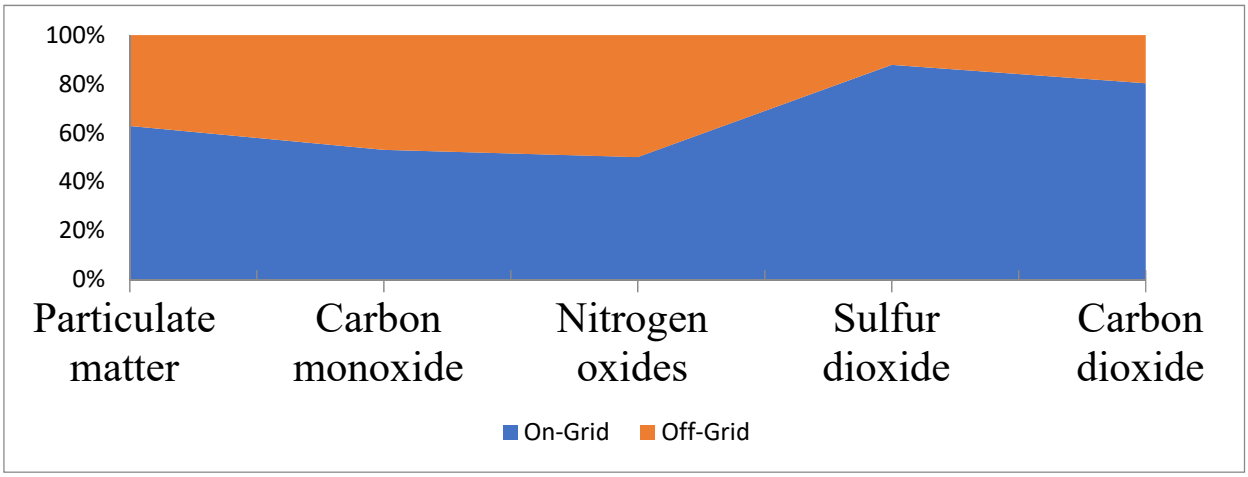

Figure 10. Contribution of GHG emission factors to optimal on-\off-grid HGEF.

Table 10 compares the usual arrangement of grid units alone and PV/diesel units with on/off-grid GHG pollution.

Table 10. The most important environmental GHG emission factors.

GHG Emission Factors (kg/Year)	Formula	PV/BG	PV/Diesel	Grid Only
Particulate matter	$PM_{2.5}$	0.00183	0.261	0.44
Carbon monoxide	CO	0.0301	4.3	4.85
Nitrogen oxides	NO_X	0.0342	4.88	4.89
Sulfur dioxide	SO_2	0	1.39	10
Carbon dioxide	CO_2	0.9305	568	2307

4.4. Sensitivity Analysis (SA)

SA provides assistance in developing the proposed optimum HGEF system for the site in question. This allows observing the effects of some input variables included in the technical and economic analysis design. To investigate their impact on the ideal system, this is accomplished by assigning these variables several values within a specific range. The project term (20 and 25 years), average yearly load need (100%, 150%, and 175%), SR global horizontal, discount and inflation rates (ranging from 0 to 8), and departure factors (0.85 and 0.95) are the key factors examined. NPC and COE are thus impacted by the evaluation of many project and resource parameters. Table 9 provides a full description of the TE-environmental factors needed for HGEF modeling and simulation.

5. Simulation Results

The performance of the suggested system is investigated and tested using MATLAB/SIMULINK software, as shown in Figure 11. Table 9 lists the configuration parameters for each component used in the suggested HGEF to achieve the load needs.

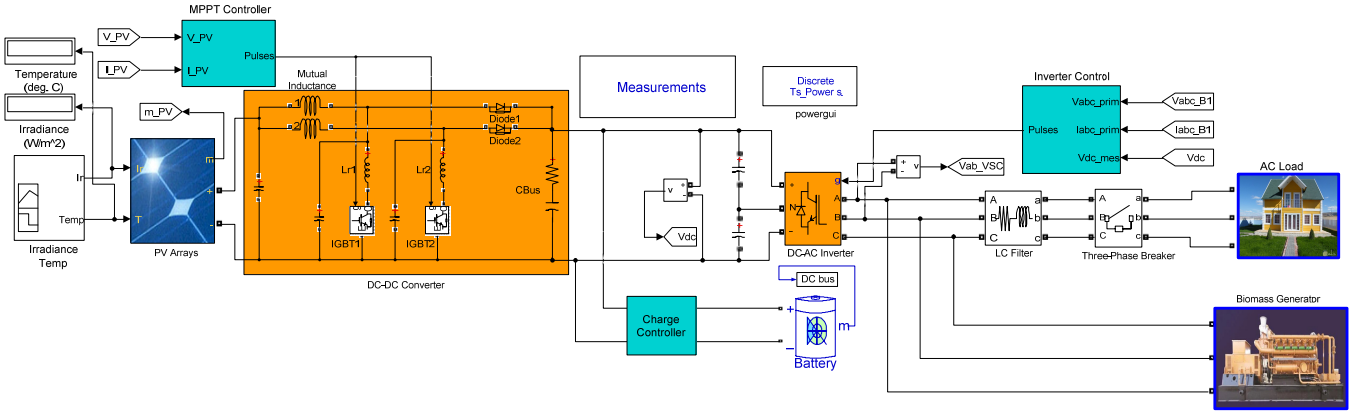

Figure 11. Investigated system.

The overall performance of a PV/BG is affected by the intensity of SR received by the PV modules and the ambient temperatures. Therefore, the input signals are converted to variable temperatures and different radiation levels to simulate system performance under more realistic environmental conditions, as shown in Figures 12 and 13. Figure 12a shows the effect of different SR levels on the V_{oc} and I_{sc} of the module under a constant temperature of 25 °C. When SR levels gradually decrease from 1000 W/m² to 200 W/m², as shown in Figure 12a, a decrease in I_{sc} occurs from (52.5 A at 1 kW/m²) to (10.51 A at 0.2 kW/m²). Moreover, the module output power is also affected, as shown in Figure 12b: the DC output power decreases by 81% from 3003 W to 569.6 W.

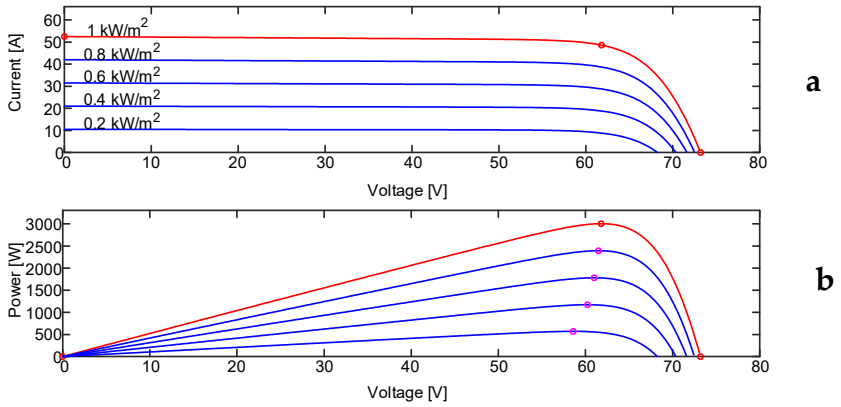

Figure 12. Characteristics of the PV curves with a constant temperature of 25 °C at different irradiance levels: (**a**) I–V curve and (**b**) P–V curve.

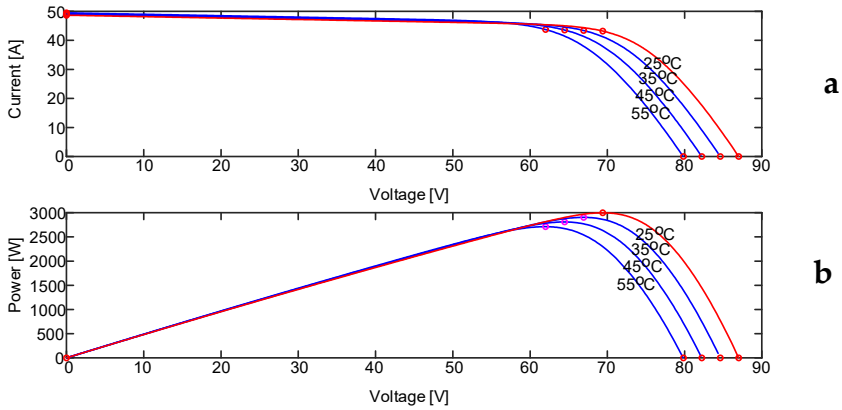

Figure 13. Characteristics of the PV curves with a constant illumination of 1000 W/m² at variable temperatures: (**a**) I–V curve and (**b**) P–V curve.

Similarly, Figure 13a shows the impact of temperature increase on both the V_{oc} and I_{sc} of the PV module under a constant illumination of 1000 W/m². When the temperature gradually rises from 25 °C to 55 °C, Isc hardly increases by 0.81 A, as shown in Figure 13a, while V_{oc} decreases from 87 V to 79.84 V. Moreover, the PV module output power is also affected, as shown in Figure 13b: the DC output power decreases by 9.6% from 2998 W to 2711 W.

Figure 14 shows the simulation results for a period of (24 h × 60 m × 60 s), i.e., throughout a full day's load and under variable temperatures and different radiation levels, which represent realistic environmental conditions. The power flow between the PVA, BG, BB, and load is shown in Figure 14. At the time point of 6.72 × 10^4 s, the load power demand increases to 3886 W, as shown in Figure 14c, which exceeds the power generated by the PVA of 1873 W at the same moment, as seen in Figure 14a. Thus, the lack of power 2013 W from the BG and BB is compensated, as shown in Figure 14b,d, which means that the power is in discharge mode, as shown in Figure 14e, in which the power produced by the PVA and BG and the power injected into the BB complement each other. At the time point of 3.96 × 10^4 s, the power demand decreases to 2279 W, as shown in Figure 14c. Energy is continuously injected into the BB because the power provided by the PVA and BG is 4534 W, as shown in Figure 13a,b, which exceeds the required load power. Thus, it is seen that the power of the BB is negative with a value of 2155 W, as shown in Figure 14d, which means that the power is being supplied (charging mode), as shown in Figure 14e.

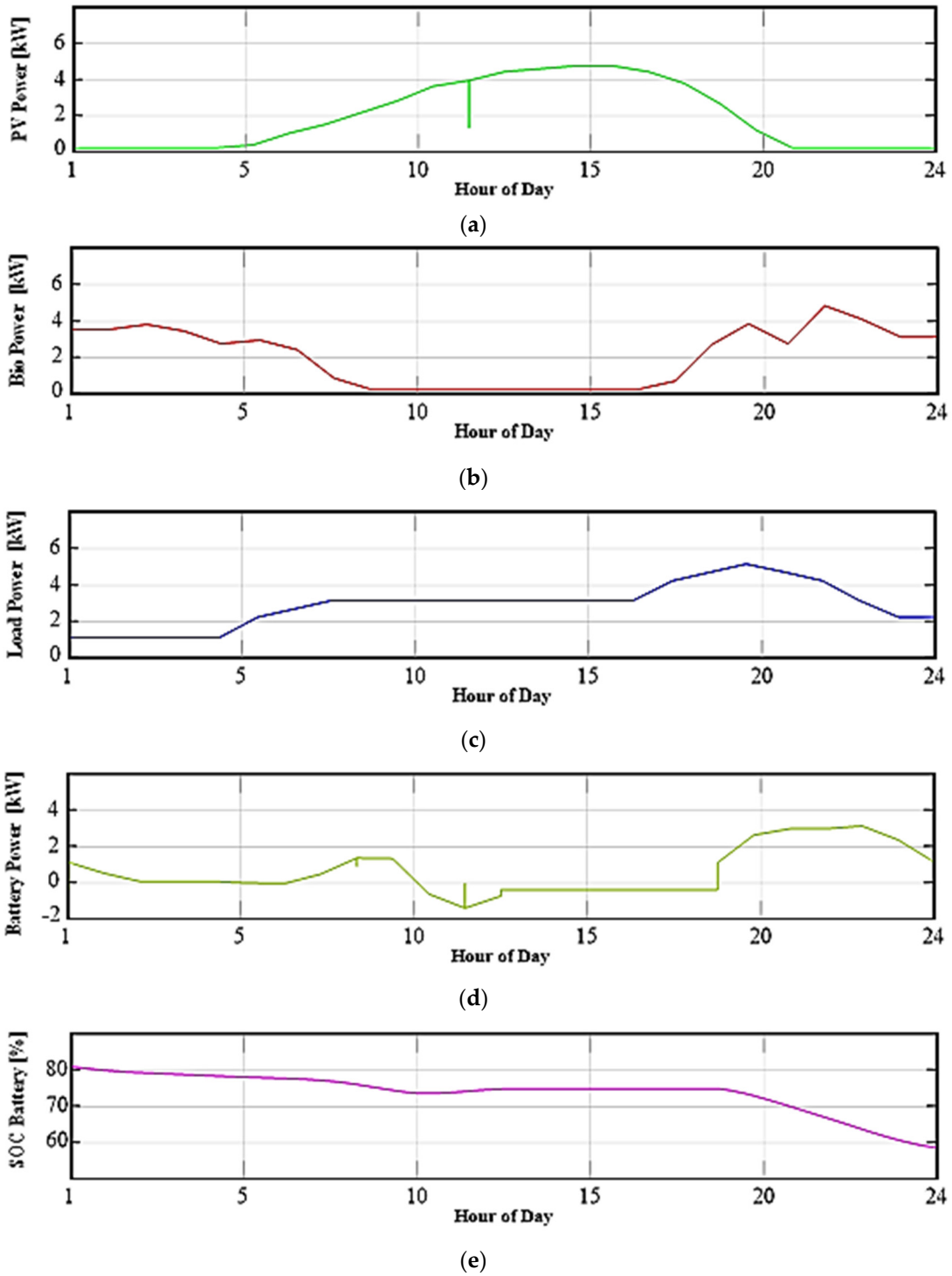

Figure 14. Power flow between the PVA, batteries, and load with variable temperatures and different radiation levels. (**a**) PV power curve, (**b**) BG power curve, (**c**) Load power curve, (**d**) BB power curve, and (**e**) SOC-BB curve.

- The proposed HGEF model attained from the HOMER program was optimally feasible and had ideal attributes for an NPC of USD 11,026, an energy generation cost of 0.346 USD/kWh, an RF of 99.9%, and a CO_2 emission of 0.9305 kg/year. The HGEF economic study revealed a payback period of 20 years and an annual real interest rate of 6% with an LCOE of 0.184 USD/kWh and an O and M cost of 50 USD/year.
- According to the previously described results, the HGEF structure involves 20 PVAs with a total DC output power of 5 kW, and a 1 kW BG with a 2 kW solar inverter to

meet all electrical loads. A storage system (lithium-ion batteries) consisting of 23 BBs with a total capacity of 612.5 Ah and a total energy of 29.4 kWh at 48 V. Depending on the required electrical loads and the amount of energy generated by the proposed HGEF, the BB is charged and discharged accordingly with a storage depletion of 0.201 kWh/year for 15 years.

- Simulation results are provided to confirm the suggested HGEF configuration using HOMER Pro and MATLAB/SIMULINK software. The simulation results show that both on-grid and off-grid HRES are economically feasible and more reliable and sustainable than using grid-based electricity or PV/DG alone.
- The grid-connected HGEF provides a more reliable, unchanging, and low-priced power supply with an energy cost of 0.18–0.28 USD/kWh. However, it depends on the location of the network infrastructure and resource capabilities and accessibility.
- In contrast, the proposed isolated HGEF offers very low annual CO_2 emissions and a more independent energy supply. Nevertheless, the price of energy production is higher (COE: 0.184 USD/kWh) due to the capacity and cost of BG and BB.

6. Conclusions

This research aims to analyze the TE-EA of an off-grid PV/BG to feed the electrical load of a house in a rural village, in Sohag Al Gadida City, Egypt. The results concluded with the following:

- According to this analysis, the PV/BG hybrid configuration is the most efficient layout out of all options to satisfy the local power need at a minimal energy price. The results also indicate that using hybrid PV/biomass is an attractive choice with the initial capital cost (ICC: USD 8.144), net present cost (NPC: USD 11.026), a low cost of energy (LCOE: 0.184 USD/kWh), and the high renewable fraction (RF: 99.9%) of the system.
- The TE-EA of various off-grid HGEF strategies relying on available local resources was studied. Furthermore, a sensitivity analysis was performed for various structures to verify the effectiveness of the optimized system even under other design constraints, such as changes in project lifetime and PV array reduction factor at different % loads.
- Consequently, the decision between the two systems ought to be based on the particular requirements and constraints of the application and its place. It is crucial to remember that combining the two systems might give Egypt access to more reliable and adaptable energy sources. Therefore, the anticipated green power production system may support both the environmental and economic well-being of the RA.

It is recommended that future research examine the viability and potential of such HGEFs in various scenarios including low-cost, large-scale storage systems, such as seasonal hydrogen storage and thermal energy storage, together with fuel cells.

Author Contributions: Conceptualization, R.K., H.S. and M.M.M.; formal analysis, A.A. and U.K.; investigation, H.S. and M.M.M.; resources, H.S. and R.K.; writing—original draft preparation, H.S. and R.K.; writing—review and editing, N.F.I., H.S. and M.M.M.; visualization, N.F.I. and H.S.; supervision, A.A., H.S., U.K. and A.B.; Funding, A.A. All authors have read and agreed to the published version of the manuscript.

Funding: This work was supported by the Researchers Supporting Project number (RSP2024R258), King Saud University, Riyadh, Saudi Arabia.

Institutional Review Board Statement: Not applicable.

Informed Consent Statement: Not applicable.

Data Availability Statement: Data are available on request from the authors.

Acknowledgments: The authors are grateful for the support by the Researchers Supporting Project number (RSP2024R258), King Saud University, Riyadh, Saudi Arabia.

Conflicts of Interest: The authors declare no conflicts of interest.

Abbreviations

AC	Alternating Current
BG	Bio-Gas
BGDG	Bio-Gas Diesel Generator
BM	Bio-Mass
BS	Battery Storage
BTUs	British Thermal Units
CRF	Capital Recovery Factor
DC	Direct Current
DG	Diesel Generator
DOA	Days of Autonomy
DOD	Depth of Discharge
EG	Energy Generation
FC	Fuel Cell
FF	Fossil Fuel
GC	Generation Cost
GE	Green Energy
GHGs	Greenhouse Gases
HFC	Hydrogen Fuel Cell
HGEF	Hybrid Green Energy Farm
HOMER	Hybrid Optimization of Multiple Energy Resources
HRES	Hybrid Renewable Energy Systems
ICC	Initial Capital Cost
LCOE	Lowest Cost of Energy
Li-Ion	Lithium Ion
MGPS	Micro Grid Power System
MPPT	Maximum Power Point Tracking
NASA	National Aeronautics and Space Administration
NPC	Net Present Cost
O and M	Operation and Maintenance
OC	Operational Cost
PV	Photovoltaic Panel
RC	Replacement Cost
RER	Renewable Energy Resource
RES	Renewable Energy Source
RF	Renewable Fraction
SE	Solar Energy
SOC	State of Charge
SR	Solar Radiation
STC	Standard Test Condition
TAC	Total Annual Cost
TV	Television
US	United States

Appendix A

Table A1. Some previously published works with location, system configurations, and a summary of results.

References No./Year	Location	Optimal Hybrid Conf.	Summary of Results
[43], 2023	Durham, Ontario	PV/WT/Nuclear	LCOE-0.26 USD/kWh.
[44], 2023	Al-Karak, Jordan	PV/WT	LCOE-0.024 USD/kWh.
[45], 2023	Chilubi Island, Zambia	PV/DG/BS	LCOE-0.182 USD/kWh.

[46], 2023	Oyo State, Nigeria	PV only	LCOE-0.1904 USD/kWh.
[47], 2023	Western Ethiopia	PV/WT/BS	LCOE-0.173 USD/kWh.
[48], 2022	Punjab, India	PV/BG	NPC-21087 USD, LCOE-0.362 USD/kWh, RF-99.9%.
[49], 2022	Gaza city	PV/BG/DG	LCOE-0.438 USD/kWh.
[50], 2022	Nankese, Ghana	PV/grid, PV/Genset	PV-Grid, LCOE-0.0824 USD/kWh. PV-Genset, LCOE-0.309 USD/kWh.
[51], 2022	Malaysia	PV/WT/BS/DG	LCOE-0.198 USD/kWh.
[52], 2022	Chintalaya Palle, A.P., India.	PV/WT/DG/BS	NPC-5.48 M USD, LCOE-0.272 USD/kWh, RF-91.6%.
[53], 2022	Diyala, Iraq	PV/FC	NPC-10,166 USD, LCOE-0.23 USD/kWh, RF-91.8%.
[54], 2022	Korkadu East, Villiyanur Commune, Puducherry, India	PV/WT/BM	NPC-Rs.573 M USD, LCOE-Rs.7.886 USD/kWh, RF-86.2%.
[55], 2021	Kanadripalle, Andhra Pradesh, India	PV/BS/DG	NPC-3,41,280 USD, LCOE-0.217 USD/kWh, RF-96.6%.
[56], 2021	Ukai, Gujarat, India	PV/WT/BG/DG	NPC-831,217 USD, LCOE-0.196 USD/kWh, RF-81.2%.
[57], 2021	North-East Indian States	PV/HFC	NPC in the range of USD (327,557–443,004), LCOE in the range of (0.509–0.689) USD/kWh, RF-100%.
[58], 2021	Korkadu, Pondicherry, India	PV/WT/BM	NPC-Rs.11.9 M USD, LCOE-Rs.8.231 USD/kWh, RF-100%.
[59], 2021	Gaharika, Kandhamal District, Odissa	WT/PV/BS	NPC-454,242 USD, LCOE-0.278 USD/kWh.
[60], 2021	14 Sites Across Gilgit-Baltistan	HG/WT/PV with DG or BS	LCOE in the range of (0.0470–0.0968) USD/kWh.
[61], 2021	Suez University, Egypt	PV/WT/BS with DG	LCOE-0.343USD/kWh.
[62], 2021	Xining, China	WT/FC/BS	NPC-59,611 USD, LCOE-1.278 USD/kWh.
[63], 2020	Yalova University, Turkey	PV/WT/DG/BS	NPC-1.77 M USD, LCOE-0.145 USD/kWh, RF-75.2%.
[64], 2020	Newcastle, UK	BGDG/WT/BS	NPC-14,507 USD, LCOE-0.588 USD/kWh, RF-82.3%.
[65], 2020	West China	PV/WT/BGDG/BS	NPC-456,388 USD, LCOE-0.206 USD/kWh.
[66], 2020	Fou ay Village, Benin Republic	PV/DG/BS	NPC-555,492 USD, LCOE-0.207 USD/kWh, RF-97.7%.
[67], 2020	Adrar, Sahara of Algeria	PV/Li-Ion/BS	NPC-27,361 USD, LCOE-0.25 USD/kWh, RF-88.3%.
[68], 2019	Jubail Industrial City, Saudi Arabia	PV/WT/DG/BS	NPC-555,492 M USD,

			LCOE-0.25 USD/kWh, RF-100%.
[69], 2019	Southern Cameroons, the Central and West African Regions	PV/DG/BS	NPC-191,700 USD, LCOE-0.443 USD/kWh, RF-100%.
[70], 2019	Diyala, Muqdadiyah District, Iraq	PV/BS/DG	NPC-110,191 USD, LCOE-0.21 USD/kWh, RF-35.6%.
[42], 2019	Eskisehir, Turkey	PV only and PV/WT/DG	LCOE in the range of (0.052–0.055) USD/kWh.

Appendix B

Table A2. Biomass production data on the cow farm at the study location.

Parameters	Value	Unit
Number of cows	8	….
Absorbing the farm of cows	12	….
Manure production per cow	12	kg/day
The length of stay in the fermenter required for the fermentation process	30	day
Cumulative production of biogas during the 30-day fermentation period	48	m^3
The highest production on the thirteenth day	4.5	m^3
The lowest production on the thirtieth day	0.5	m^3
The average daily production of biogas	1.6	m^3

References

1. Rebollal, D.; Carpintero-Rentería, M.; Santos-Martín, D.; Chinchilla, M. Microgrid and distributed energy resources standards and guidelines review: Grid connection and operation technical requirements. *Energies* **2021**, *14*, 523. https://doi.org/10.3390/en14030523.
2. Xiao, W.; Ozog, N.; Dunford, W.G. Topology study of photovoltaic interface for maximum power point tracking. *IEEE Ind. Electron. Mag.* **2007**, *54*, 1696–1704. https://doi.org/10.1109/tie.2007.894732.
3. Awad, M.; Said, A.; Saad, M.H.; Farouk, A.; Mahmoud, M.M.; Alshammari, M.S.; Alghaythi, M.L.; Aleem, S.H.A.; Abdelaziz, A.Y.; Omar, A.I. A review of water electrolysis for green hydrogen generation considering PV/wind/hybrid/hydropower/geothermal/tidal and wave/biogas energy systems, economic analysis, and its application. *Alex. Eng. J.* **2024**, *87*, 213–239. https://doi.org/10.1016/j.aej.2023.12.032.
4. Dağtekin, M.; Kaya, D.; Öztürk, H.H.; Kiliç, F.C. A study of techno-economic feasibility analysis of solar photovoltaic (PV) power generation in the province of Adana in Turkey. *Energy Explor. Exploit.* **2014**, *32*, 719–735. https://doi.org/10.1260/0144-5987.32.4.719.
5. Mahmoud, M.M. Improved current control loops in wind side converter with the support of wild horse optimizer for enhancing the dynamic performance of PMSG-based wind generation system. *Int. J. Model. Simul.* **2023**, *43*, 952–966. https://doi.org/10.1080/02286203.2022.2139128.
6. Semeskandeh, S.; Hojjat, M.; Abardeh, M.H. Techno–economic–environmental feasibility study of a photovoltaic system in northern part of Iran including a two-stage multi-string inverter with DC–DC ZETA converter and a modified P&O algorithm. *Clean Energy* **2022**, *6*, 127–140. https://doi.org/10.1093/ce/zkab057.
7. Mahmoud, M.M.; Atia, B.S.; Esmail, Y.M.; Bajaj, M.; Wapet, D.E.M.; Ratib, M.K.; Hossain, B.; AboRas, K.M.; Abdel-Rahim, A.-M.M. Evaluation and Comparison of Different Methods for Improving Fault Ride-Through Capability in Grid-Tied Permanent Magnet Synchronous Wind Generators. *Int. Trans. Electr. Energy Syst.* **2023**, *2023*, 7717070. https://doi.org/10.1155/2023/7717070.
8. Elmi, Y.K.; Jazayeri, M.; Salman, D. The feasibility of economic viability of hybrid PV-diesel energy system connect with the main grid in Somalia. *Int. J. Smart Grid Clean Energy* **2022**, *11*. https://doi.org/10.12720/sgce.11.2.83-91.
9. Kassem, Y.; Gökçekuş, H.; Güvensoy, A. Techno-economic feasibility of grid-connected solar pv system at near east university hospital, northern cyprus. *Energies* **2021**, *14*, 7627. https://doi.org/10.3390/en14227627.
10. Olówósejéjé, S.; Leahy, P.; Morrison, A.P. Optimising photovoltaic-centric hybrid power systems for energy autonomy. *Energy Rep.* **2021**, *7*, 1943–1953. https://doi.org/10.1016/j.egyr.2021.03.039.
11. Ibrahim, N.F.; Alkuhayli, A.; Beroual, A.; Khaled, U.; Mahmoud, M.M. Enhancing the Functionality of a Grid-Connected Photovoltaic System in a Distant Egyptian Region Using an Optimized Dynamic Voltage Restorer: Application of Artificial Rabbits Optimization. *Sensors* **2023**, *23*, 7146. https://doi.org/10.3390/s23167146.

12. El Maysse, I.; El Magri, A.; Watil, A.; Alkuhayli, A.; Kissaoui, M.; Lajouad, R.; Giri, F.; Mahmoud, M.M. Nonlinear Observer-Based Controller Design for VSC-Based HVDC Transmission Systems Under Uncertainties. *IEEE Access* **2023**, *11*, 124014–124030. https://doi.org/10.1109/access.2023.3330440.
13. Channi, H.K. Techno Economic Feasibility Analysis of Solar PV System in Jammu: A Case Study. In *Solar Cells-Theory, Materials and Recent Advances*; IntechOpen: London, UK, 2021. https://doi.org/10.5772/intechopen.98809.
14. Ibrahim, N.F.; Mahmoud, M.M.; Alnami, H.; Wapet, D.E.M.; Ardjoun, S.A.E.M.; Mosaad, M.I.; Hassan, A.M.; Abdelfattah, H. A new adaptive MPPT technique using an improved INC algorithm supported by fuzzy self-tuning controller for a grid-linked photovoltaic system. *PLoS ONE* **2023**, *18*, e0293613. https://doi.org/10.1371/journal.pone.0293613.
15. Zayed, M.E.; Zhao, J.; Li, W.; Elsheikh, A.H.; Elaziz, M.A. A hybrid adaptive neuro-fuzzy inference system integrated with equilibrium optimizer algorithm for predicting the energetic performance of solar dish collector. *Energy* **2021**, *235*, 121289. https://doi.org/10.1016/j.energy.2021.121289.
16. Jahangiri, M.; Haghani, A.; Shamsabadi, A.A.; Mostafaeipour, A.; Pomares, L.M. Feasibility study on the provision of electricity and hydrogen for domestic purposes in the south of Iran using grid-connected renewable energy plants. *Energy Strat. Rev.* **2019**, *23*, 23–32. https://doi.org/10.1016/j.esr.2018.12.003.
17. Khan, M.J.; Yadav, A.K.; Mathew, L. Techno economic feasibility analysis of different combinations of PV-Wind-Diesel-Battery hybrid system for telecommunication applications in different cities of Punjab, India. *Renew. Sustain. Energy Rev.* **2017**, *76*, 577–607. https://doi.org/10.1016/j.rser.2017.03.076.
18. Kamel, O.M.; Diab, A.A.Z.; Mahmoud, M.M.; Al-Sumaiti, A.S.; Sultan, H.M. Performance Enhancement of an Islanded Microgrid with the Support of Electrical Vehicle and STATCOM Systems. *Energies* **2023**, *16*, 1577. https://doi.org/10.3390/en16041577.
19. Dehghan, M.; Pfeiffer, C.F.; Rakhshani, E.; Bakhshi-Jafarabadi, R. A review on techno-economic assessment of solar water heating systems in the middle east. *Energies* **2021**, *14*, 4944. https://doi.org/10.3390/en14164944.
20. Abubakr, H.; Vasquez, J.C.; Mahmoud, K.; Darwish, M.M.F.; Guerrero, J.M. Comprehensive Review on Renewable Energy Sources in Egypt—Current Status, Grid Codes and Future Vision. *IEEE Access* **2022**, *10*, 4081–4101. https://doi.org/10.1109/access.2022.3140385.
21. Hani, E.H.B.; Sinaga, N.; Khanmohammdi, S.; Diyoke, C. Assessment of a waste energy recovery (WER) unit for power and refrigeration generation: Advanced thermodynamic examination. *Sustain. Energy Technol. Assess.* **2022**, *52*, 102213. https://doi.org/10.1016/j.seta.2022.102213.
22. Hermann, D.T.; Donatien, N.; Armel, T.K.F.; René, T. Techno-economic and environmental feasibility study with demand-side management of photovoltaic/wind/hydroelectricity/battery/diesel: A case study in Sub-Saharan Africa. *Energy Convers. Manag.* **2022**, *258*, 115494. https://doi.org/10.1016/j.enconman.2022.115494.
23. Avila, D.; Marichal, G.N.; Hernández, Á.; Luis, F.S. Hybrid renewable energy systems for energy supply to autonomous desalination systems on Isolated Islands. In *Design, Analysis and Applications of Renewable Energy Systems*; Academic Press: Cambridge, MA, USA, 2021; pp. 23–51. https://doi.org/10.1016/B978-0-12-824555-2.00009-5.
24. Shaahid, S.; El-Amin, I. Techno-economic evaluation of off-grid hybrid photovoltaic–diesel–battery power systems for rural electrification in Saudi Arabia—A way forward for sustainable development. *Renew. Sustain. Energy Rev.* **2009**, *13*, 625–633. https://doi.org/10.1016/j.rser.2007.11.017.
25. Khalil, A.K.; Mubarak, A.M.; Kaseb, S.A. Road map for renewable energy research and development in Egypt. *J. Adv. Res.* **2010**, *1*, 29–38. https://doi.org/10.1016/j.jare.2010.02.003.
26. Attia, S.; De Herde, A. Sizing photovoltaic systems during early design: A decision tool for architects. In Proceedings of the ASES 2010—39th Annual American National Solar Energy Conference, Phoenix, Arizona, 17–22 May June 2010; pp. 5186–5212.
27. Palenzuela, P.; Alarcónpadilla, D.C.; Zaragoza, G.; Blanco, J. Comparison between CSP+MED and CSP+RO in Mediterranean Area and MENA Region: Techno-economic Analysis. *Energy Procedia* **2015**, *69*, 1938–1947. https://doi.org/10.1016/j.egypro.2015.03.192.
28. Trieb, F. Trans-Mediterranean Interconnection for Concentrating Solar Power. In Proceedings of the Synergistic Supergrid Conference, London, UK, 19–21 January 2010; pp. 1–22.
29. Gad, H.E.; El-Gayar, S.M. Performance prediction of a proposed photovoltaic water pumping system at South Sinai, Egypt climate conditions. In Proceedings of the Thirteenth International Water Technology Conference, IWTC13 2009, Hurghada, Egypt, 12–15 March 2009; Volume 13, pp. 739–752.
30. Taha, A.T.H. Estimation of hourly global solar radiation in egypt using mathematical model. *Misr J. Agric. Eng.* **2010**, *27*, 2033–2047. https://doi.org/10.21608/mjae.2010.105401.
31. Abo-Khalil, A.G.; Abo-Zied, H. Modelling and simulation of a grid-connected photovoltaic system for an middle-class apartment in new assiut city. *JES. J. Eng. Sci.* **2012**, *40*, 1747–1757. https://doi.org/10.21608/jesaun.2012.114617.
32. Abdel-Rehim, Z.S.; Lasheen, A. Experimental and theoretical study of a solar desalination system located in Cairo, Egypt. *Desalination* **2007**, *217*, 52–64. https://doi.org/10.1016/j.desal.2007.01.012.
33. Patchali, T.E.; Ajide, O.O.; Matthew, O.J.; Salau, T.A.O.; Oyewola, O.M. Examination of potential impacts of future climate change on solar radiation in Togo, West Africa. *SN Appl. Sci.* **2020**, *2*, 1941. https://doi.org/10.1007/s42452-020-03738-3.
34. Salim, M.G. Selection of groundwater sites in Egypt, using geographic information systems, for desalination by solar energy in order to reduce greenhouse gases. *J. Adv. Res.* **2012**, *3*, 11–19. https://doi.org/10.1016/j.jare.2011.02.008.

35. Mandal, S.; Das, B.K.; Hoque, N. Optimum sizing of a stand-alone hybrid energy system for rural electrification in Bangladesh. *J. Clean. Prod.* **2018**, *200*, 12–27. https://doi.org/10.1016/j.jclepro.2018.07.257.
36. Jahangir, M.H.; Shahsavari, A.; Rad, M.A.V. Feasibility study of a zero emission PV/Wind turbine/Wave energy converter hybrid system for stand-alone power supply: A case study. *J. Clean. Prod.* **2020**, *262*, 121250. https://doi.org/10.1016/j.jclepro.2020.121250.
37. Sayed, K.; El Zohri, E.H.; Mahfouz, H. Analysis and design for interleaved ZCS buck DC-DC converter with low switching losses. *Int. J. Power Electron.* **2017**, *8*, 210. https://doi.org/10.1504/ijpelec.2017.085076.
38. Markovic, D.; Cvetkovic, D.; Masic, B. Survey of software tools for energy efficiency in a community. *Renew. Sustain. Energy Rev.* **2011**, *15*, 4897–4903. https://doi.org/10.1016/j.rser.2011.06.014.
39. Fikri, M.A.; Samykano, M.; Pandey, A.; Kadirgama, K.; Kumar, R.R.; Selvaraj, J.; Rahim, N.A.; Tyagi, V.; Sharma, K.; Saidur, R. Recent progresses and challenges in cooling techniques of concentrated photovoltaic thermal system: A review with special treatment on phase change materials (PCMs) based cooling. *Sol. Energy Mater. Sol. Cells* **2022**, *241*, 111739. https://doi.org/10.1016/j.solmat.2022.111739.
40. Horne, S. 10—Concentrating Photovoltaic (CPV) Systems and Applications. BT—Concentrating Solar Power Technology. In *Concentrating Solar Power Technology*; Woodhead Publishing Series in Energy; Woodhead Publishing: Sawston, UK, 2012; pp. 323–361. Available online: http://www.sciencedirect.com/science/article/pii/B9781845697693500108 (accessed on 22 January 2024).
41. Turkdogan, S. Design and optimization of a solely renewable based hybrid energy system for residential electrical load and fuel cell electric vehicle. *Eng. Sci. Technol. Int. J.* **2021**, *24*, 397–404. https://doi.org/10.1016/j.jestch.2020.08.017.
42. Çetinbaş, I.; Tamyürek, B.; Demirtaş, M. Design, analysis and optimization of a hybrid microgrid system using homer software: Eskişehir osmangazi university example. *Int. J. Renew. Energy Dev.* **2019**, *8*, 65–79. https://doi.org/10.14710/ijred.8.1.65-79.
43. Gabbar, H.A.; Siddique, A.B. Technical and economic evaluation of nuclear powered hybrid renewable energy system for fast charging station. *Energy Convers. Manag. X* **2023**, *17*, 100342. https://doi.org/10.1016/j.ecmx.2022.100342.
44. Al Afif, R.; Ayed, Y.; Maaitah, O.N. Feasibility and optimal sizing analysis of hybrid renewable energy systems: A case study of Al-Karak, Jordan. *Renew. Energy* **2023**, *204*, 229–249. https://doi.org/10.1016/j.renene.2022.12.109.
45. Mulenga, E.; Kabanshi, A.; Mupeta, H.; Ndiaye, M.; Nyirenda, E.; Mulenga, K. Techno-economic analysis of off-grid PV-Diesel power generation system for rural electrification: A case study of Chilubi district in Zambia. *Renew. Energy* **2023**, *203*, 601–611. https://doi.org/10.1016/j.renene.2022.12.112.
46. Amole, A.O.; Oladipo, S.; Olabode, O.E.; Makinde, K.A.; Gbadega, P. Analysis of grid/solar photovoltaic power generation for improved village energy supply: A case of Ikose in Oyo State Nigeria. *Renew. Energy Focus* **2023**, *44*, 186–211. https://doi.org/10.1016/j.ref.2023.01.002.
47. Benti, N.E.; Mekonnen, Y.S.; Asfaw, A.A. Combining green energy technologies to electrify rural community of Wollega, Western Ethiopia. *Sci. Afr.* **2023**, *19*, e01467. https://doi.org/10.1016/j.sciaf.2022.e01467.
48. Kumar, R.; Channi, H.K. A PV-Biomass off-grid hybrid renewable energy system (HRES) for rural electrification: Design, optimization and techno-economic-environmental analysis. *J. Clean. Prod.* **2022**, *349*, 131347. https://doi.org/10.1016/j.jclepro.2022.131347.
49. Al-Najjar, H.; El-Khozondar, H.J.; Pfeifer, C.; Al Afif, R. Hybrid grid-tie electrification analysis of bio-shared renewable energy systems for domestic application. *Sustain. Cities Soc.* **2022**, *77*, 103538. https://doi.org/10.1016/j.scs.2021.103538.
50. Asamoah, S.S.; Gyamfi, S.; Uba, F.; Mensah, G.S. Comparative assessment of a stand-alone and a grid-connected hybrid system for a community water supply system: A case study of Nankese community in the eastern region of Ghana. *Sci. Afr.* **2022**, *17*, e01331. https://doi.org/10.1016/j.sciaf.2022.e01331.
51. See, A.M.K.; Mehranzamir, K.; Rezania, S.; Rahimi, N.; Afrouzi, H.N.; Hassan, A. Techno-economic analysis of an off-grid hybrid system for a remote island in Malaysia: Malawali island, Sabah. *Renew. Sustain. Energy Transit.* **2022**, *2*, 100040. https://doi.org/10.1016/j.rset.2022.100040.
52. Pujari, H.K.; Rudramoorthy, M. Optimal design, prefeasibility techno-economic and sensitivity analysis of off-grid hybrid renewable energy system. *Int. J. Sustain. Energy* **2022**, *41*, 1466–1498. https://doi.org/10.1080/14786451.2022.2058502.
53. Hassan, Q.; Jaszczur, M.; Hafedh, S.A.; Abbas, M.K.; Abdulateef, A.M.; Hasan, A.; Abdulateef, J.; Mohamad, A. Optimizing a microgrid photovoltaic-fuel cell energy system at the highest renewable fraction. *Int. J. Hydrogen Energy* **2022**, *47*, 13710–13731. https://doi.org/10.1016/j.ijhydene.2022.02.108.
54. Pandiyan, P.; Sitharthan, R.; Saravanan, S.; Prabaharan, N.; Tiwari, M.R.; Chinnadurai, T.; Yuvaraj, T.; Devabalaji, K. A comprehensive review of the prospects for rural electrification using stand-alone and hybrid energy technologies. *Sustain. Energy Technol. Assess.* **2022**, *52*, 102155. https://doi.org/10.1016/j.seta.2022.102155.
55. Pujari, H.K.; Rudramoorthy, M. Optimal design and techno-economic analysis of a hybrid grid-independent renewable energy system for a rural community. *Int. Trans. Electr. Energy Syst.* **2021**, *31*, e13007. https://doi.org/10.1002/2050-7038.13007.
56. Sawle, Y.; Jain, S.; Babu, S.; Nair, A.R.; Khan, B. Prefeasibility Economic and Sensitivity Assessment of Hybrid Renewable Energy System. *IEEE Access* **2021**, *9*, 28260–28271. https://doi.org/10.1109/access.2021.3058517.
57. Pal, P.; Mukherjee, V. Off-grid solar photovoltaic/hydrogen fuel cell system for renewable energy generation: An investigation based on techno-economic feasibility assessment for the application of end-user load demand in North-East India. *Renew. Sustain. Energy Rev.* **2021**, *149*, 111421. https://doi.org/10.1016/j.rser.2021.111421.

58. Krishnamoorthy, M.; Saisandeep, M.; Balasubramanian, K.; Srinivasan, S.; Thaniaknti, S.B. Techno economic performance analysis of hybrid renewable electrification system for remote villages of India. *Int. Trans. Electr. Energy Syst.* **2021**, *31*, e12515. https://doi.org/10.1002/2050-7038.12515.
59. Sahu, P.K.; Jena, S.; Sahoo, U. Techno-Economic Analysis of Hybrid Renewable Energy System with Energy Storage for Rural Electrification. In *Hybrid Renewable Energy Systems*; Scrivener Publishing LLC: Beverly, MA, USA, 2021; pp. 63–96. https://doi.org/10.1002/9781119555667.ch3.
60. Ali, M.; Wazir, R.; Imran, K.; Ullah, K.; Janjua, A.K.; Ulasyar, A.; Khattak, A.; Guerrero, J.M. Techno-economic assessment and sustainability impact of hybrid energy systems in Gilgit-Baltistan, Pakistan. *Energy Rep.* **2021**, *7*, 2546–2562. https://doi.org/10.1016/j.egyr.2021.04.036.
61. Elnozahy, A.; Yousef, A.M.; Ghoneim, S.S.M.; Abdelwahab, S.A.M.; Mohamed, M.; Abo-Elyousr, F.K. Optimal Economic and Environmental Indices for Hybrid PV/Wind-Based Battery Storage System. *J. Electr. Eng. Technol.* **2021**, *16*, 2847–2862. https://doi.org/10.1007/s42835-021-00810-9.
62. Li, C. Technical and economic potential evaluation of an off-grid hybrid wind-fuel cell-battery energy system in Xining, China. *Int. J. Green Energy* **2021**, *18*, 258–270. https://doi.org/10.1080/15435075.2020.1854267.
63. Kiliç, G.A.; Al, K.; Dağtekin, E.; Ünver, Ü. Technical, economic and environmental investigation of grid-independent hybrid energy systems applicability: A case study. *Energy Sources Part A Recovery Util. Env.* **2020**, 1–16. https://doi.org/10.1080/15567036.2020.1825565.
64. Miao, C.; Teng, K.; Wang, Y.; Jiang, L. Technoeconomic analysis on a hybrid power system for the uk household using renewable energy: A case study. *Energies* **2020**, *13*, 3231. https://doi.org/10.3390/en13123231.
65. Li, J.; Liu, P.; Li, Z. Optimal design and techno-economic analysis of a solar-wind-biomass off-grid hybrid power system for remote rural electrification: A case study of west China. *Energy* **2020**, *208*, 118387. https://doi.org/10.1016/j.energy.2020.118387.
66. Odou, O.D.T.; Bhandari, R.; Adamou, R. Hybrid off-grid renewable power system for sustainable rural electrification in Benin. *Renew. Energy* **2020**, *145*, 1266–1279. https://doi.org/10.1016/j.renene.2019.06.032.
67. Mokhtara, C.; Negrou, B.; Bouferrouk, A.; Yao, Y.; Settou, N.; Ramadan, M. Integrated supply–demand energy management for optimal design of off-grid hybrid renewable energy systems for residential electrification in arid climates. *Energy Convers. Manag.* **2020**, *221*, 113192. https://doi.org/10.1016/j.enconman.2020.113192.
68. Baseer, M.; Alqahtani, A.; Rehman, S. Techno-economic design and evaluation of hybrid energy systems for residential communities: Case study of Jubail industrial city. *J. Clean. Prod.* **2019**, *237*, 117806. https://doi.org/10.1016/j.jclepro.2019.117806.
69. Muh, E.; Tabet, F. Comparative analysis of hybrid renewable energy systems for off-grid applications in Southern Cameroons. *Renew. Energy* **2019**, *135*, 41–54. https://doi.org/10.1016/j.renene.2018.11.105.
70. Aziz, A.S.; Tajuddin, M.F.N.; Adzman, M.R.; Mohammed, M.F.; Ramli, M.A. Feasibility analysis of grid-connected and islanded operation of a solar PV microgrid system: A case study of Iraq. *Energy* **2020**, *191*, 116591. https://doi.org/10.1016/j.energy.2019.116591.